

ENVELOPE SOLITON IN WEAKLY DESSIPATIVE DUSTY PLASMA

Maria Mutahir

Layout

- **Introduction:**

⇒ Plasma ⇒ Fourth state of matter ⇒ Plasma around Us ⇒ Dusty plasma

⇒ Linear/Nonlinear waves

⇒ The mathematical model

(1st 2nd and 3rd order of ϵ . ⇒ NLS ⇒ Plots)

- **Conclusion:**

⇒ Decision and reflection of the result.

- **References:**

PLASMA

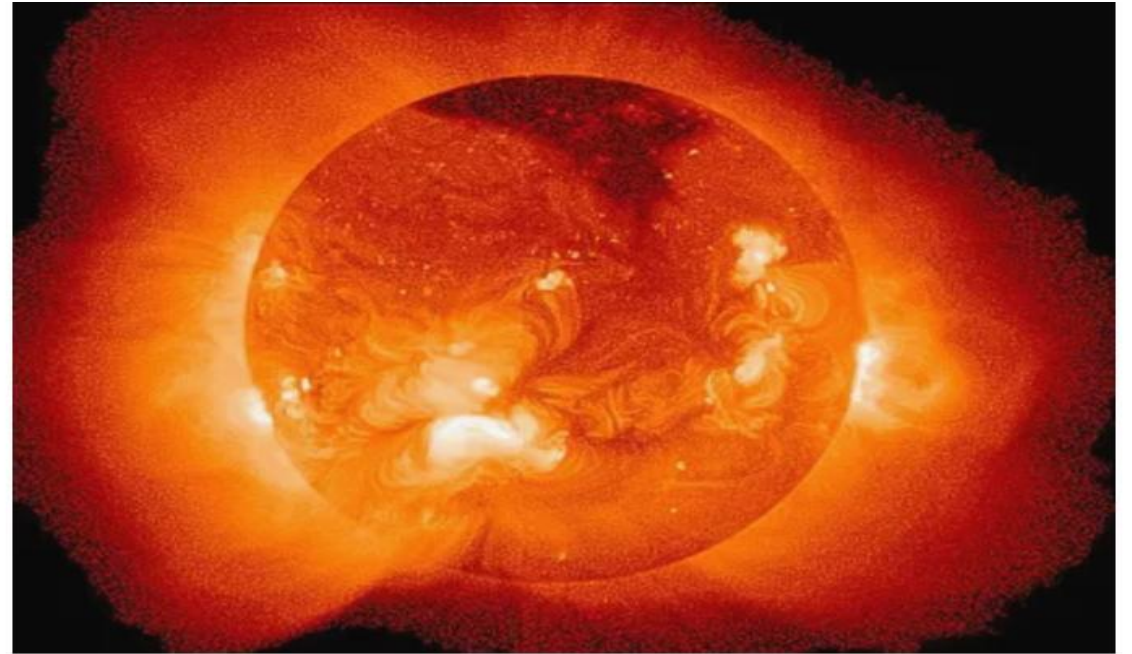
- Introduces the state of matter that resembles a gas but has certain unique properties.
- Plasma comes Greek which means something molded.
- 99.9% of all visible matter in the universe exist in the state of plasma.
- Gases turn into plasma as they reach a thermal heat and ionize.
- Plasma is a superheated matter in which a gas-like substances consisting of particles such as positive ions and electrons.
- Partially or fully ionized space plasmas have the usually the same number of positive (ions) and negative (electrons) charges and therefore behave quasineutral.


Fourth state of matter

Matter can exist in other than the three property recognizes states solid, liquid and gas. The plasma state is a medium comprising positive and negative particles and ions (mainly ions form) that is charge-neutral overall. Instead of engaging with surrounding approximately equal numbers of positively charged ions and negatively charged electrons. The characteristics of plasma are significantly different from those of ordinary neutral gases so that plasmas are considered as distinct “Fourth state of matter”

Plasma around us

- The sun and other stars consist of plasma. Plasma is also found naturally in lightning and in the northern and southern lights.
- Plasma consist of charged particles called ions, so it conducts electric current and glows when electricity passes through it. So that's why plasma is used in artificial lights.



 This is a view of the sun from the Soft X-Ray Telescope (SXT) on the Yohkoh satellite. The looping structures consist of hot plasma bound by magnetic field lines. Sunspots would be found at the base of these loops. NASA Goddard Laboratory

- Human made plasmas are found in fluorescent lights, plasma TV screens and Plasma shperes.

- In the night sky, plasma glows in the form of stars, nebulas, and in the auroras.



📷 Aurora Borealis, or Northern Lights, above Bear Lake, Eielson Air Force Base, Alaska. The colors of the aurora derive from the emission spectra of ionized gases in the atmosphere. United States Air Force photo by Senior Airman Joshua Strang

- Neon signs along the city streets are made up of plasma.



- Fireballs are discharge phenomena in ionized low temperature plasmas.



📷 The electrical discharge of lightning exists in the form of plasma. Charles Allison, Oklahoma Lightning

Dusty plasma

A dusty plasma contains tiny charged particles of dust (typically found in space). The dust particles acquire high charges and interact with each other. A plasma that contains larger particles is called grain plasma.

A dust grains can be either negatively or positively charged and mostly in astrophysical and laboratory negatively charged polarity are observed. However in some of the space, plasma regimes for example in the upper portion of the ionosphere or in the lower portion of the magnetosphere in which (the dust number density ranges observ ~ 10 to 100 cm^{-3} and dust size ranges from ~ 0.1 to $1 \mu\text{m}$), dust of positive charge polarity are also observed.

Dusty plasma are interesting because presence of particles significantly alters the charged particle equilibrium leading to different phenomena. It is a field of current research. Electrostatic coupling between the grains can vary over a wide range so that the states of the dusty plasma can change from weakly coupled (gaseous) to crystalline. Such plasmas are of interest as non-Hamiltonian system of interacting particles and as a means to study generic fundamental physics of self-organization pattern formation, phase transition and scaling.

As we know that plasma include comets, planetary rings, exposed dusty surface etc but we have also some man made plasma which are Rocket exhaust, Dust on surface in space, Dust in fusion devices thermonuclear fireballs and in some laboratories and technologies. Also the temperature of dust in a plasma may be quite different from its environment.

Linear waves

Linear waves are described by linear equations, i.e those where in each term of equation the dependent variable and its derivative are at most first degree. This means that the superposition principle applies and linear combinations of simple solutions can be used to form more complex solution.

Nonlinear waves

Non linear waves are described by nonlinear equations, and therefore superposition principle does not generally apply. Generally three types of nonlinearities are studied in plasma

1. Scalar type nonlinearities (e.g solitons or solitary waves, solitons envelope etc)
2. Vector or rotational type nonlinearities (e.g vortices etc)
3. Chaotic evolution of instabilities.

Solitons

Solitons are nonlinear waves. A soliton is considered as solitary wave solution of

nonlinear partial differential equation (PDE). A soliton is a localized wave solution of

a nonlinear PDE which is remarkably stable. One PDE that has such a solution is the

Korteweg-deVries (KdV) equation. Which are stable and do not disperse with time.

Normalized model equations

Plasma composed of dust and electrons\ions

$$\frac{\partial n_d}{\partial t} + \nabla \cdot (n_d \mathbf{v}_d) = 0, \quad (6)$$

$$\frac{\partial}{\partial t} \mathbf{v}_d + \mathbf{v}_d \cdot \nabla \mathbf{v}_d = \nabla \Phi - \nu \mathbf{v}_d, \quad (7)$$

$$\nabla \Phi = \frac{1}{2\sigma_i} \nabla n_e^{2/3}, \quad (8)$$

$$\nabla \Phi = -\frac{1}{2} \nabla n_i^{2/3}, \quad (9)$$

$$\nabla^2 \Phi = \delta_e n_e - \delta_i n_i + n_d, \quad (10)$$

First order in ε : first harmonic and dispersion relation

Let's begin with $l=1$ and $n=1$, i.e the first harmonic in the first order of perturbation.

$$v_{d1}^{(1)} = -\frac{\omega}{k} \Phi_1^{(1)}, \quad n_{d1}^{(1)} = -\frac{\omega^2}{k^2} \Phi_1^{(1)}, \quad (16)$$

$$n_{e1}^{(1)} = 3\sigma_i \Phi_1^{(1)}, \quad n_{i1}^{(1)} = -3\Phi_1^{(1)}, \quad (17)$$

The poisson equation of first order in ε as

$$\Phi_1^{(1)} = \delta_e n_{e1}^{(1)} - \delta_i n_{i1}^{(1)} + n_{d1}^{(1)}, \quad (18)$$

Substituting the first harmonic and first order perturbation densities in the poisson equation, we obtained following dispersion relation:

$$\omega^2 = \frac{k^2}{k^2 + \alpha}, \quad (19)$$

The Havnes function (h) dependant phase speed can be easily resorted in following way from equation (19).

$$v_p = \sqrt{\frac{1}{\alpha}}. \quad (20)$$

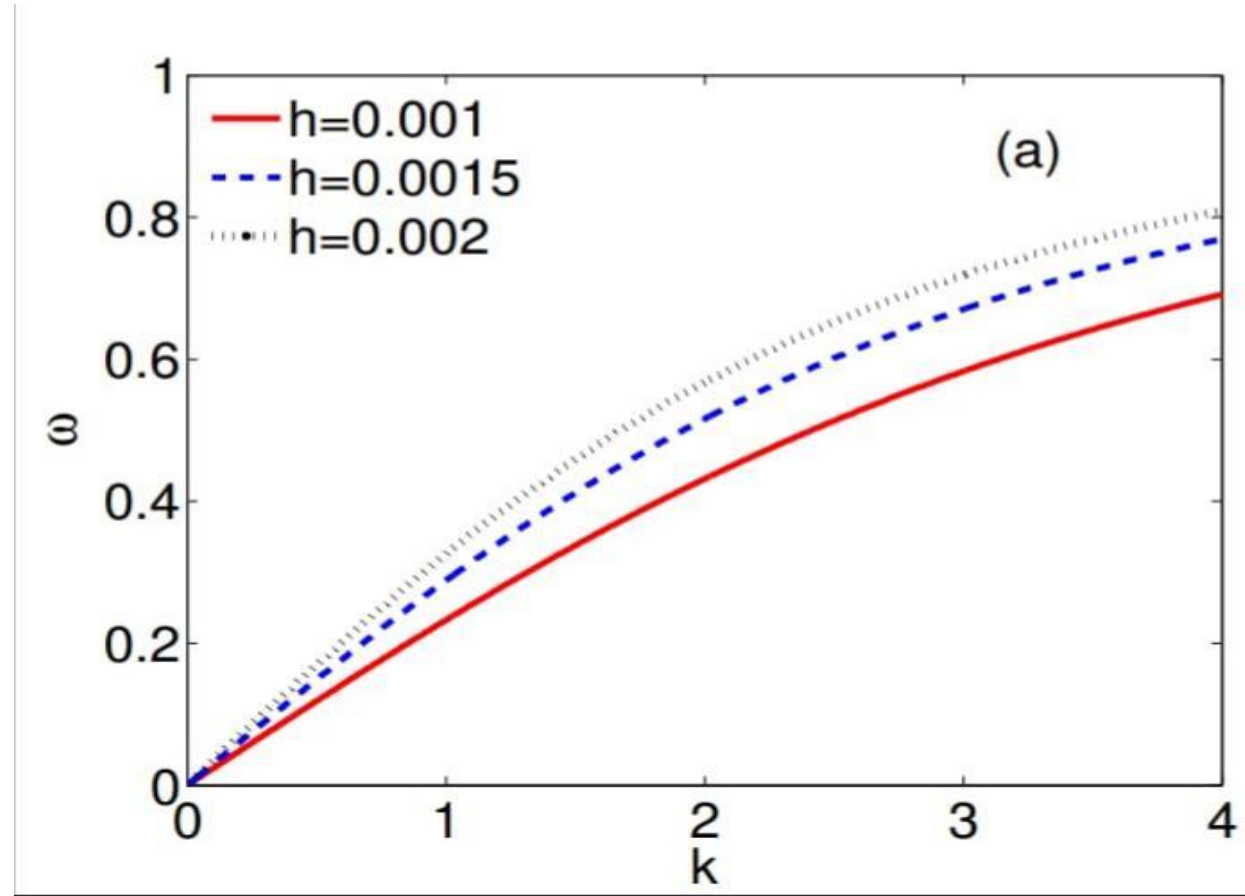


FIG. 1: Dispersion curves are depicted in Fig(a) angular frequency ω (normalized by ω_{pd}) versus the wave number k (normalized by λ_d for three different values of Havnes function (h) for $n_{e0} = 2 \times 10^{27} \text{ cm}^{-3}$, $n_{d0} = 10^{18} \text{ cm}^{-3}$ and $Z_d = 10^3$.

The equation of dispersion (19) can be written as a physical units (dimensional) form as:

$$\omega^2 = \frac{\omega_{pd}^2 k^2}{k^2 + \left(\lambda_{d,eff}^h\right)^{-2}}, \quad (21)$$

where,

$$\lambda_{d,eff}^h = \frac{\lambda_d}{\sqrt{\alpha}}, \quad (22)$$

$$c_d^h = c_d \sqrt{\alpha}. \quad (23)$$

Above Eqs. is called h-dependant effective Debye screening length effective acoustic speed and show that the process of the charge screening is affected by the Havnes function (h). The effective Debye length $\lambda_{d,eff}^h$ reduced to zero when $h \rightarrow 0$

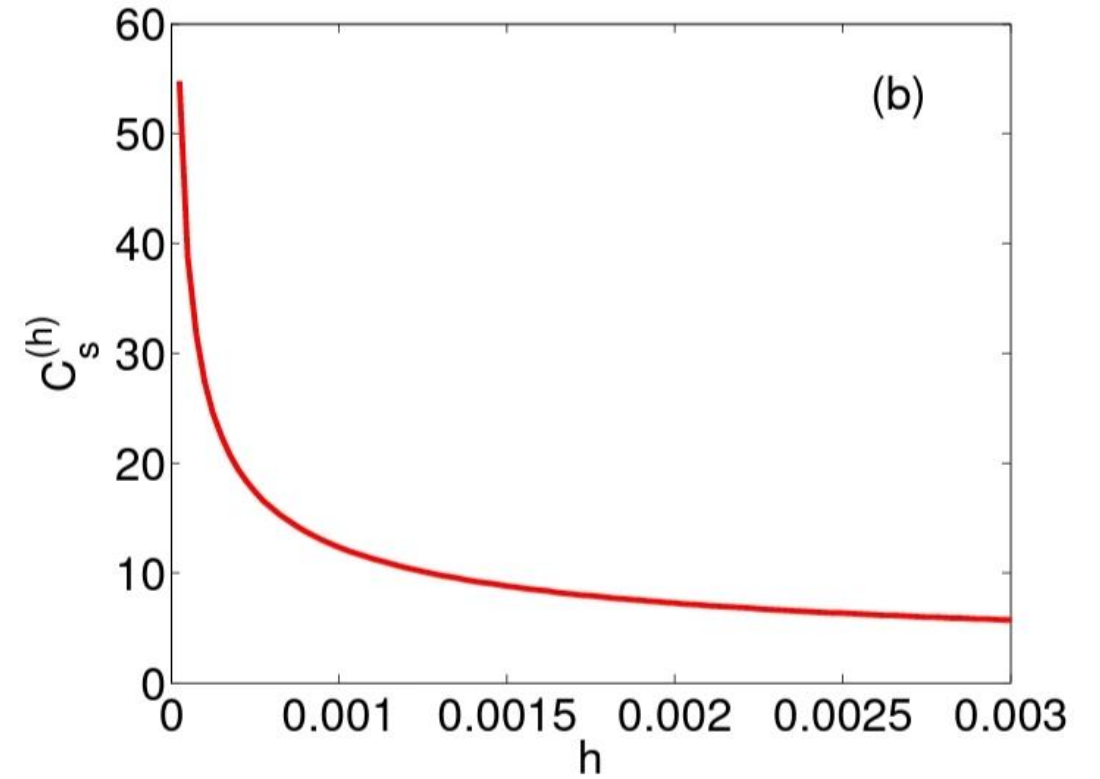
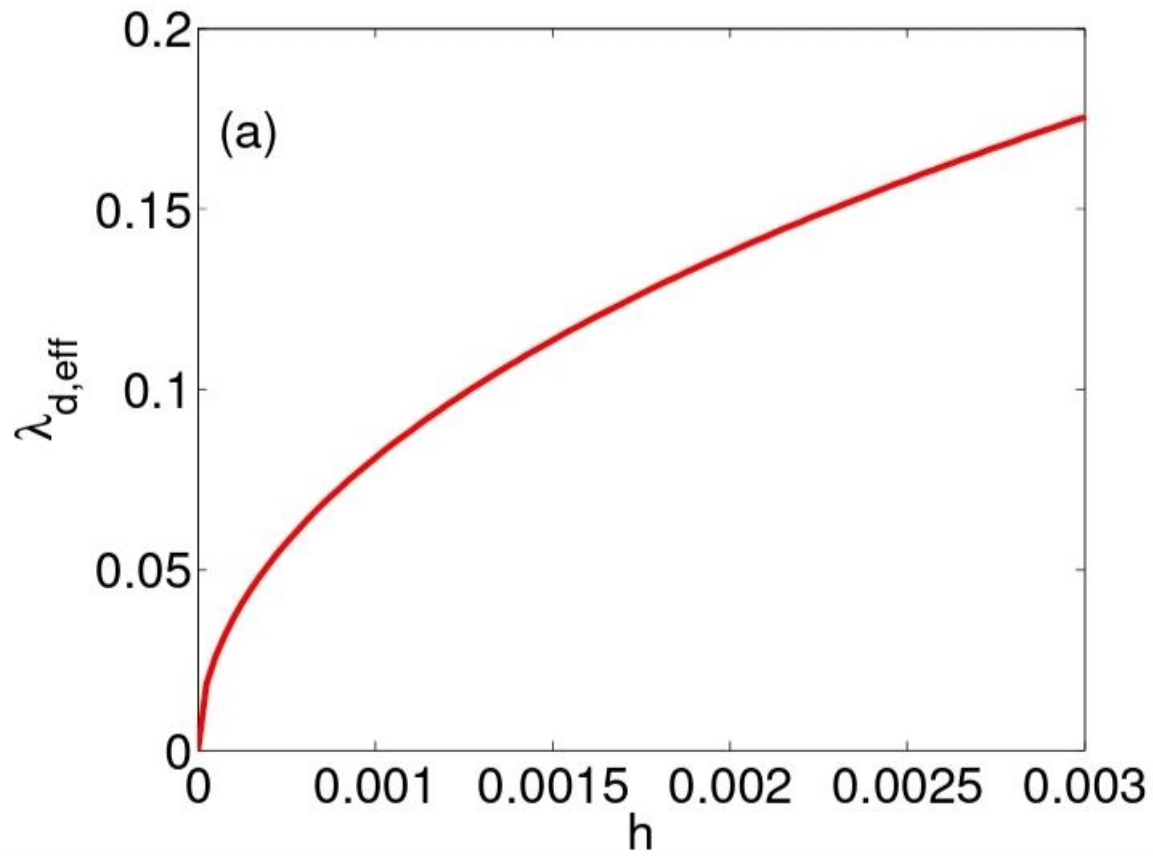


FIG. 2: Effective charge screening length λ_d^{eff} (scaled by λ_d) and the h depended sound like acoustic speed $c_d^{(h)}$ (scaled by c_d) are plotted versus the Havnes function (h), in Fig(a) effective charge screening length λ_d^{eff} and Fig(b) h depended sound like acoustic speed $c_d^{(h)}$, all other parameters are same as in 1.

3rd order and derivation of the nonlinear Schrodinger equation

we replace $l=1$ and $n=3$ and putting previous developed expressions for various variables, we get the nonlinear Schrodinger equation as follow:

$$i \frac{\partial}{\partial \tau} \Phi + P \frac{\partial^2}{\partial \xi^2} \Phi + Q \Phi |\Phi|^2 + i\Gamma \Phi = 0, \quad (38)$$

For simplicity $\Phi_1^{(1)} = \Phi$, where P is the group dispersion coefficient Γ is the dissipative coefficient, and Q is nonlinearty coefficient.

Linear oscillatory solution and modulation instability of DA waves

Now we turn to the linear MI of oscillatory wave investigation solutions for the dissipative NLS equation (38). First of all, we notice that's Eq (38) holding the following solution for a plane wave:

$$\Phi^0(\xi, \tau) = \Phi_0 \exp\left(\varphi_0(\xi, \tau)\right), \quad (41)$$

$$\varphi_0(\xi, \tau) = i \left(k_0 \xi - k_0^2 P \tau - \frac{1}{2\Gamma} Q |\Phi_0|^2 \exp[2\gamma\tau] \right) \quad (42)$$

leads the following linearized time-dependant frequency $\Omega(\tau)$

$$\Omega = \left(-i\Gamma \pm PK \sqrt{K^2 - 2\frac{Q}{P} |\Phi_0|^2 \exp[-2\Gamma\tau]} \right) \quad (46)$$

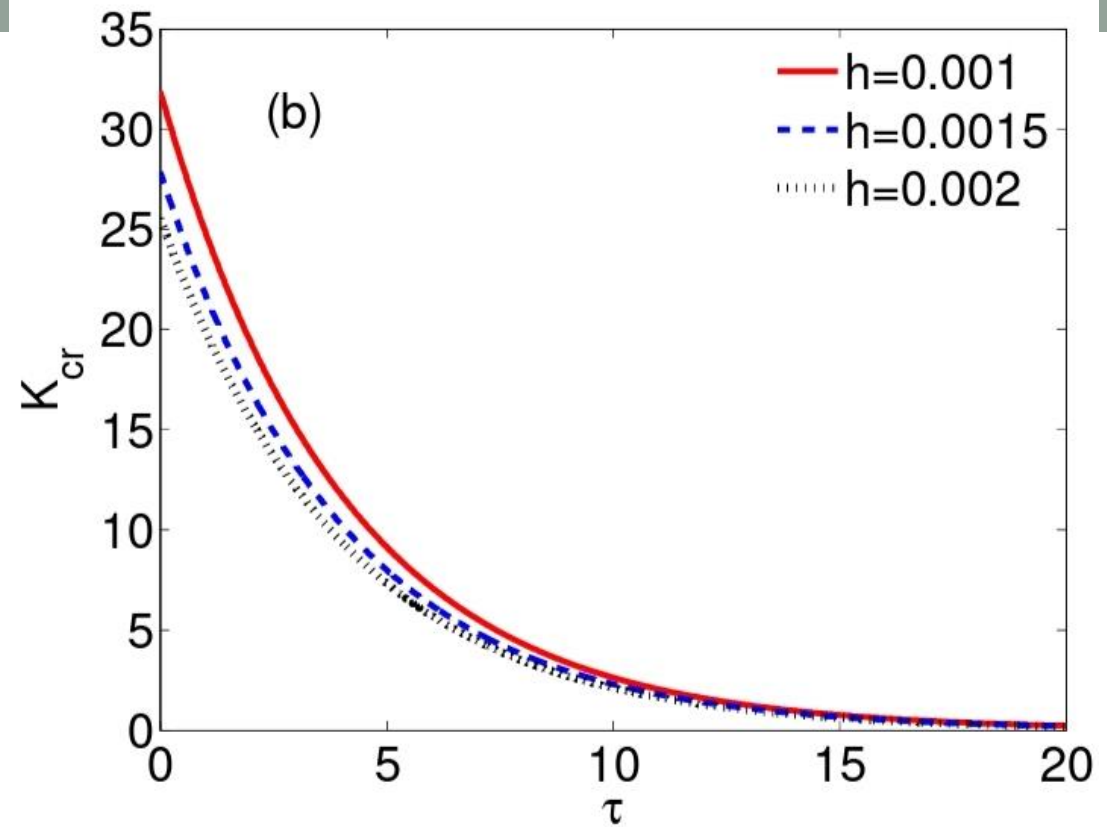
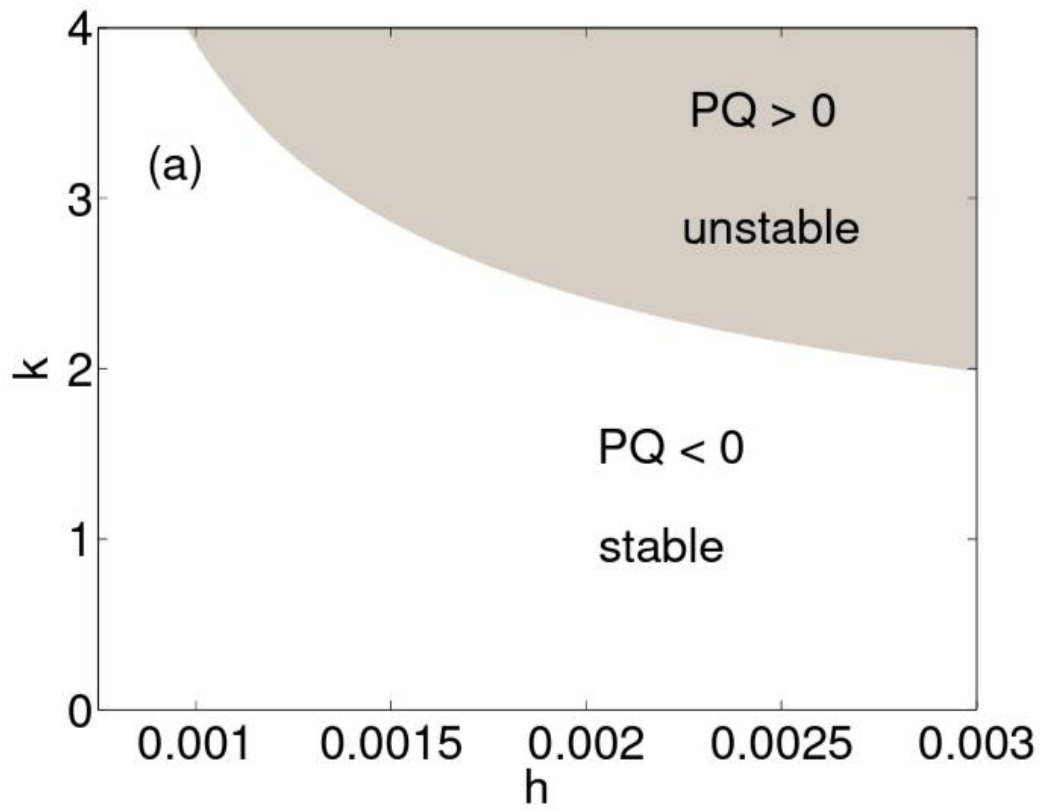


FIG. 3: The modulation instability region are depicted, in plot (a) contour plot of the product PQ on the (h,k) plane and plot (b) critical value of K_{cr} versus time τ for three different value of h and all other parameters are same as in 1.

It is evident from Eq. (46) that for negative values of PQ i.e. $PQ < 0$, the time-dependant frequency $\Omega(\tau)$ will be real function of for any wavenumber K of the perturbation and oscillatory wave solution (41) will be stable on modulation. Conversely, with a positive value of PQ i.e. $PQ > 0$ then the time-dependant frequency $\Omega(\tau)$ would keep a nonzero real value. Instability sets for K below the critical value i.e. for wavelengths above a threshold frequency wavelength defining the instability growth rate by the following relation:

$$\gamma = PK \sqrt{2 \frac{Q}{P} |\Phi_0|^2 \exp[-2\Gamma\tau] - K^2}. \quad (47)$$

As Kc decreases exponentially with time τ , the rate of instability γ decreases with time in case ($PQ > 0$). As a result there is also time limit to observe MI instability τ_{max} maximum time above that MW completely damped and instability will cease. To observe instability the time must be $\tau < \tau_{max}$ where maximum time τ_{max} can be calculated from Eq (46)

$$\tau_{max} = \frac{1}{2\Gamma} \ln \left(\frac{2PQK^2 |\Phi_0|^2}{\Gamma^2 + P^2K^2} \right) \quad (48)$$

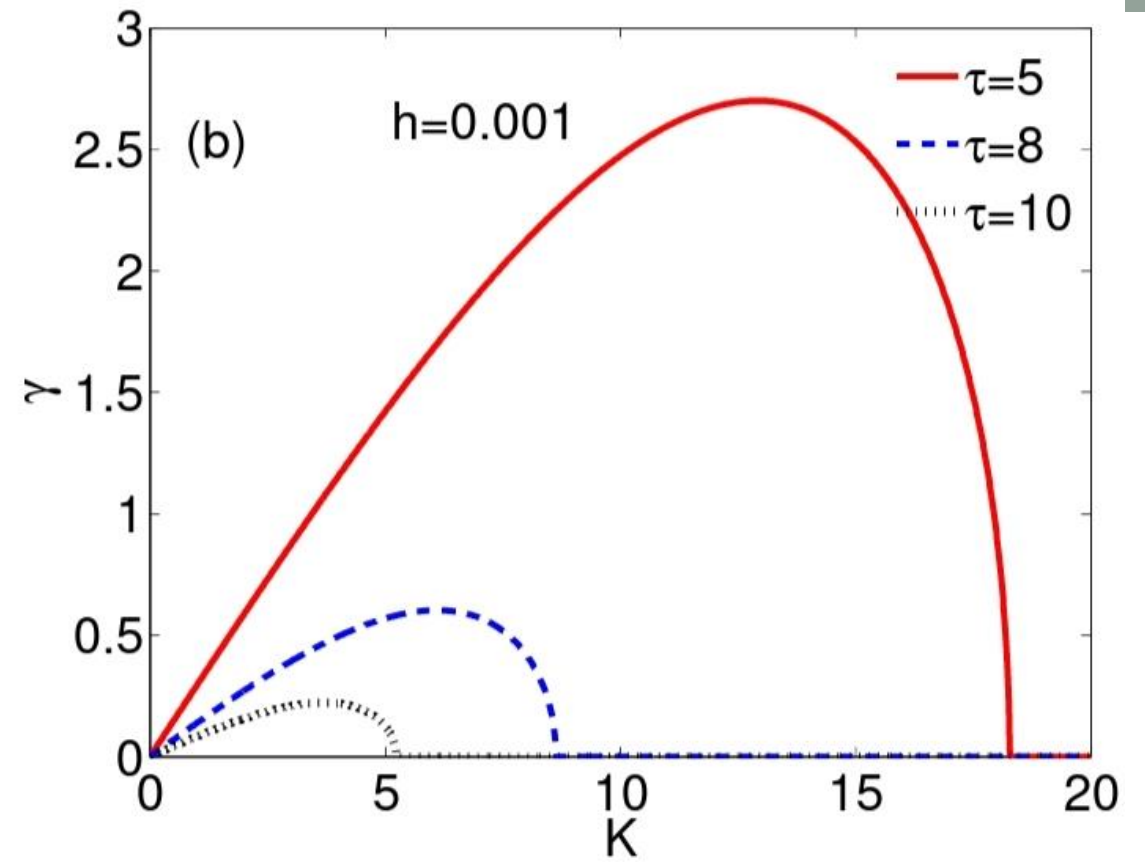
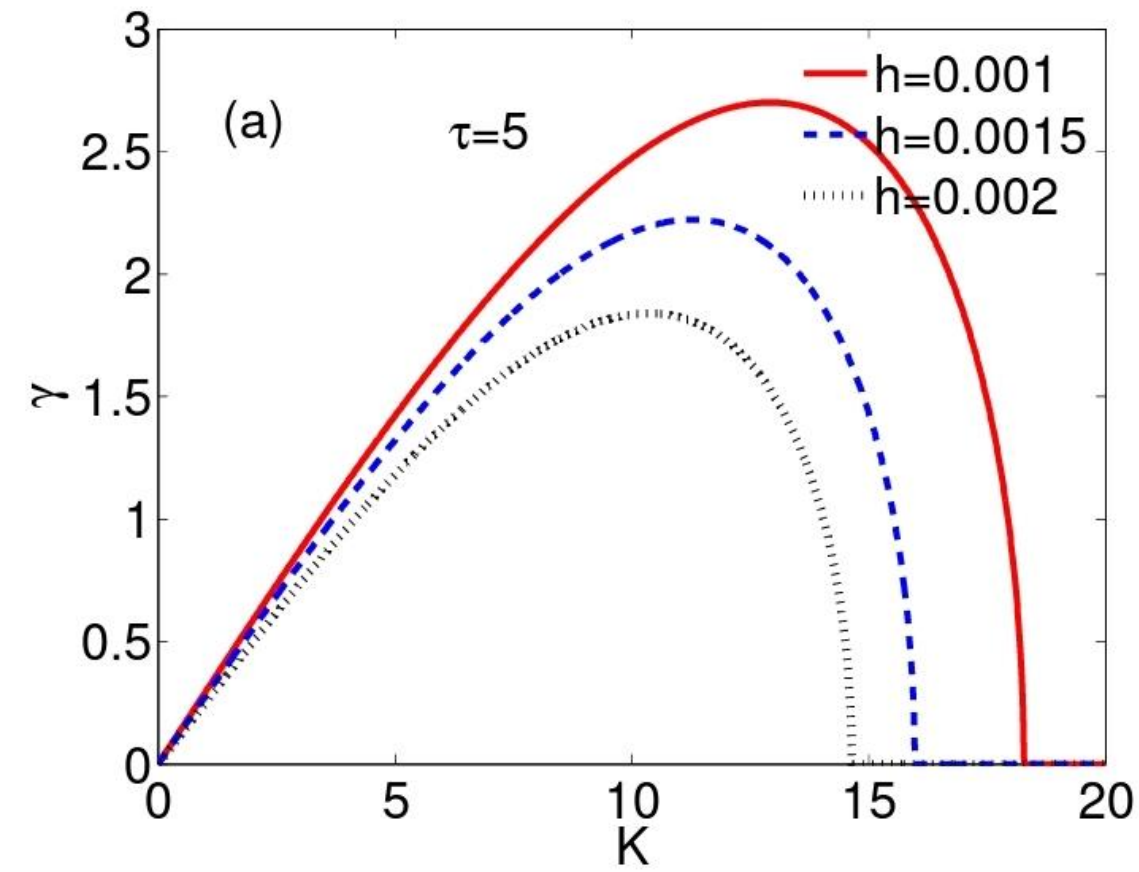


FIG. 4: The growth rates of modulation instability γ are plotted with respect to the modulational wavenumber K for a fixed values of $k = 2.5$ (a) Havnes function h effects are depicted with $\tau = 5$ and (b) the effect of $\tau = 5$ with $h = 0.001$ and all other parameters are same as in Fig.1.

Modulated envelope solitons

Here we calculate the existence of modulated envelope solitons. The dissipative nonlinear Schrodinger equation (38) allows the appearances of localized pulses in the form of modulated envelope solitons of either bright or dark type, depending upon the sign of the product PQ or of the ratio Q/P .

Bright envelope solitons

When the product of PQ or P/Q ratio is positive i.e. $PQ > 0$ or $P/Q > 0$ then bright envelope solitons will be formed. In this case amplitude and phase are given by the following equations:

$$\rho(\xi, \tau) = \rho_0 \operatorname{sech}^2 \frac{(\xi - v\tau)}{L}, \quad (49)$$

$$\Theta(\xi, \tau) = \frac{1}{2P} \left(v\xi - \left(\Omega_0 + \frac{1}{2}v^2 \right) \tau \right), \quad (50)$$

In the case of when coefficient of dissipation is not equal to zero then dissipative bright envelope solitons write in the following equation:

$$\Phi(\xi, \tau) = a_0 \exp[-2\Gamma\tau] \cosh^{-1} \times \left[a_0 \exp[-2\Gamma\tau] \sqrt{\frac{Q}{2P}} (\xi + \sqrt{\frac{2P}{Q}} x_0 \tau) \right] \times \exp \left[i \sqrt{\frac{Q}{2P}} \left(x_0 \xi + \sqrt{\frac{PQ}{2}} \left(x_0^2 \tau + a_0^2 \frac{\exp(-4\Gamma\tau) - 1}{4\Gamma} \right) \right) \right]. \quad (51)$$

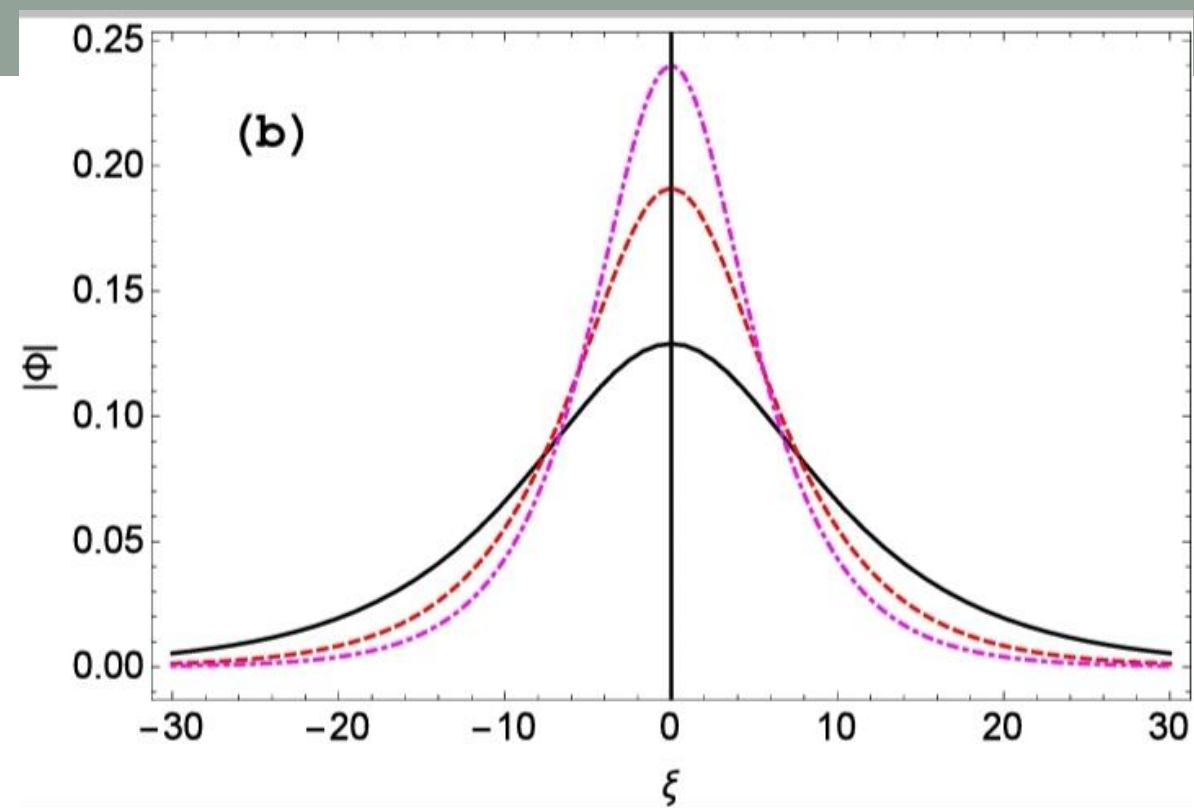
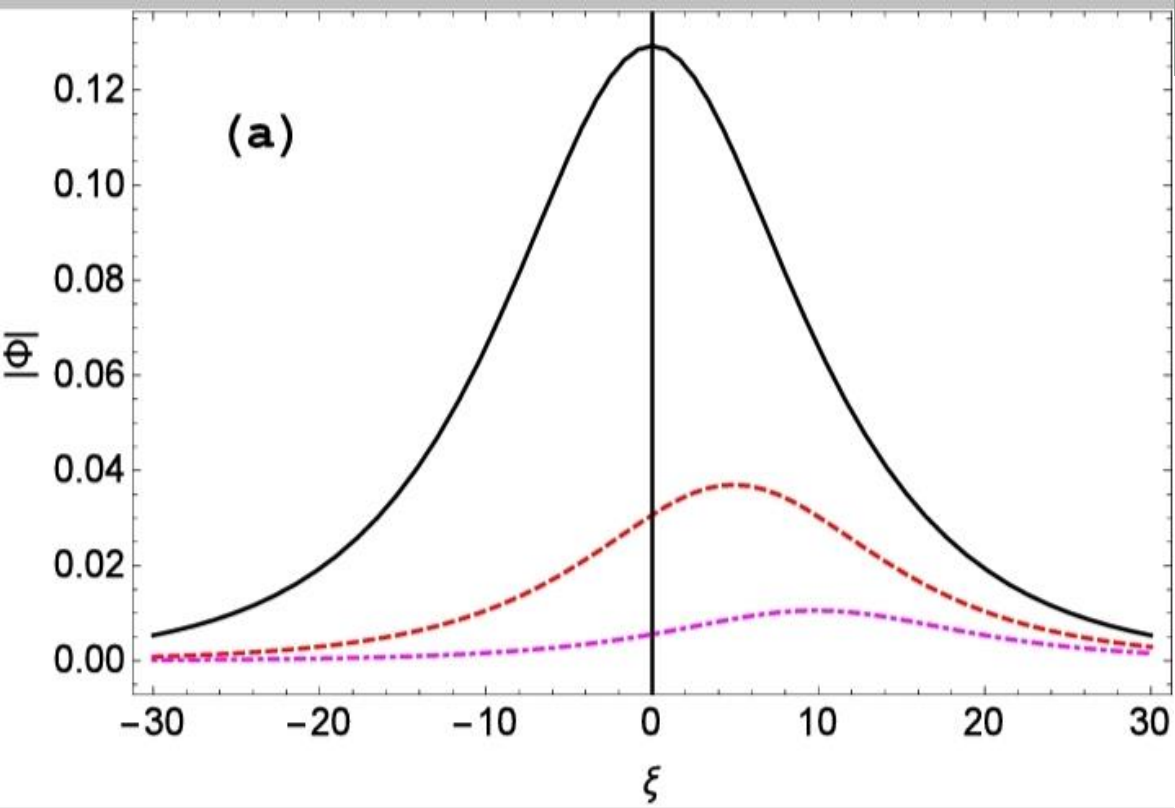


FIG. 5: Bright single solitons are plotted (a) in presence of weak collision $\Gamma = .05$ of Eq. (38) for three different time interval, solid-line $\tau = 0.1$, dashed-line $\tau = 5$ dashed-dotted-line $\tau = 10$ and (b) in the case when $\Gamma = 0$, for solid line $h = 0.001$, dashed line $h = 0.0015$, dashed-dotted line $h = 0.002$.

Dark envelope solitons

When PQ product or the ratio of P and Q is negative i.e. $PQ < 0$ or $P/Q < 0$ then the dark type solitons are formed. In this case the amplitude and phase are determined by the following equations in the absence of $\Gamma = 0$

$$\rho(\xi, \tau) = \tilde{\rho}_0 \tanh^2 \frac{(\xi - v\tau)}{\tilde{L}}, \quad (52)$$

$$\Theta(\xi, \tau) = \frac{1}{2P} \left(v\xi - \left(\frac{1}{2}v^2 - 2PQ\tilde{\rho}_0 \right) T \right), \quad (53)$$

But when dissipative if coefficient is not equal to zero we have the following dark type solitons:

$$\Phi(\xi, \tau) = u_0(\tau) \left(\eta(\tau) \tanh(\zeta(\tau)) + i\sqrt{1 - \eta^2(\tau)} \right) \exp[iQu_0^2(\tau)\tau], \quad (54)$$

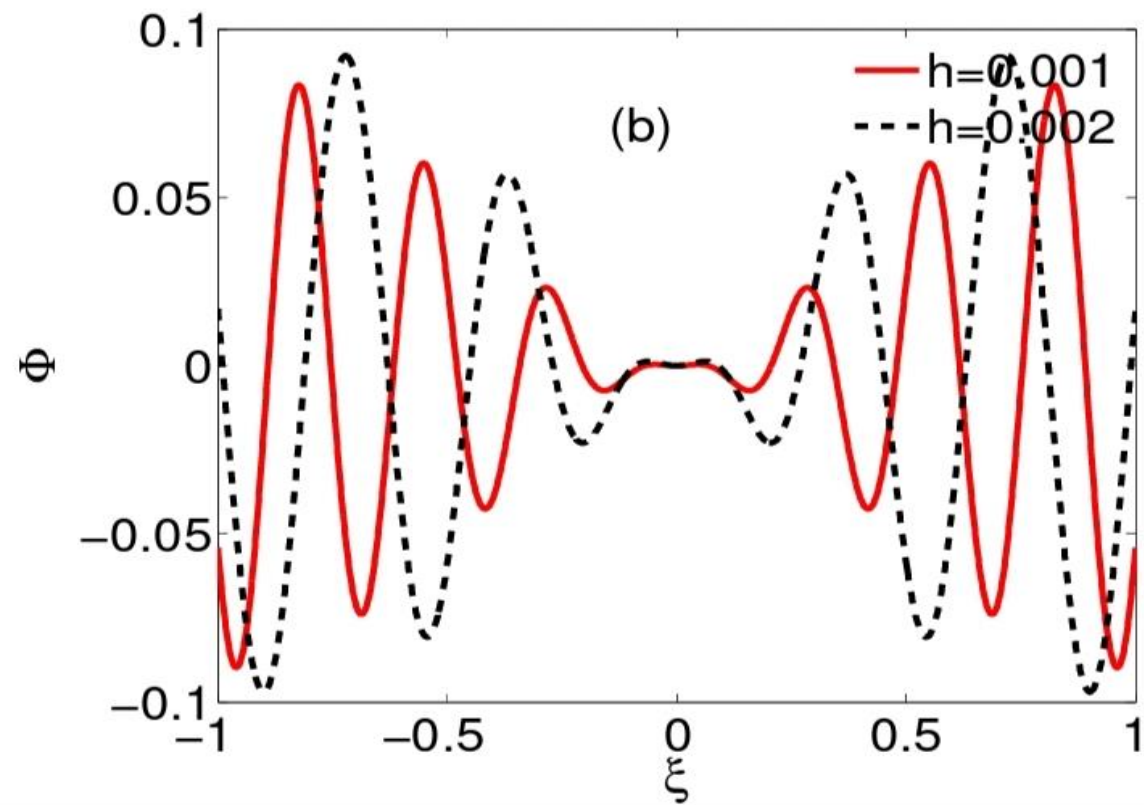
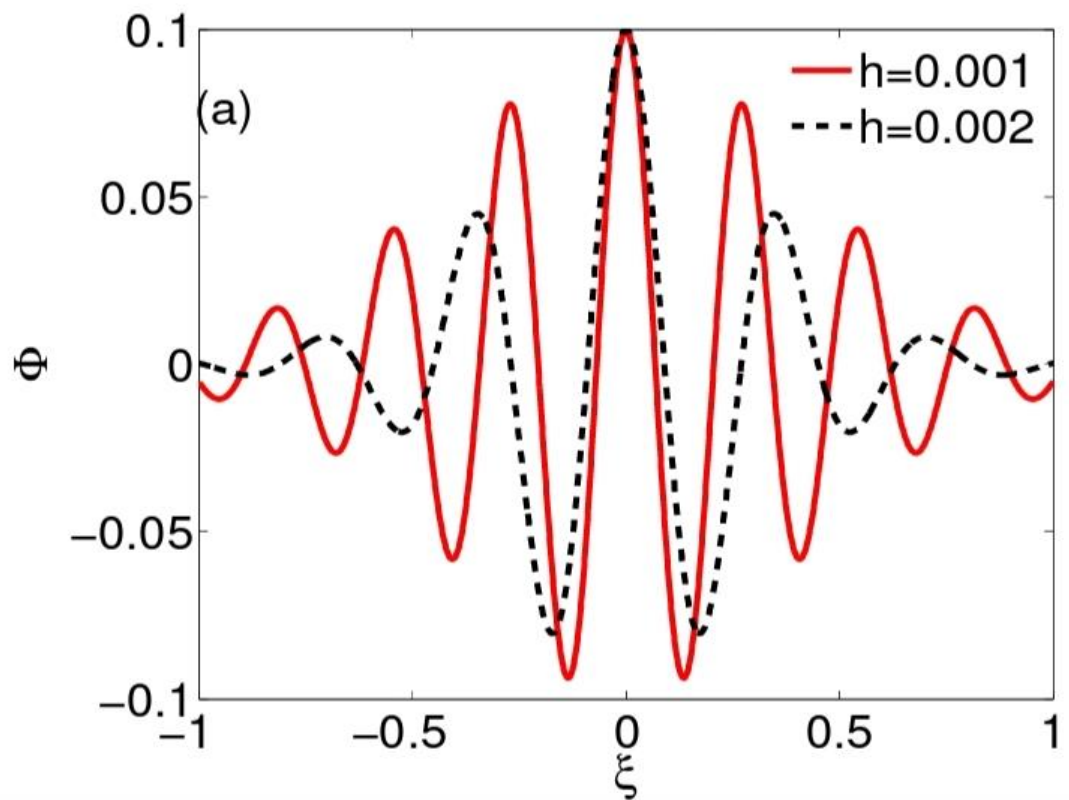


FIG. 6: Bright (a) and dark (b) envelope solitons are plotted when $\Gamma = 0$, showing the h effects on the profile of these solitons for solid line $h = 0.001$ and dashed line $h = 0.002$.

Rogue waves solution of dissipative NLS equation

In order to demonstrate and explain rogue waves solution of NLS equation (38) in the region of ($PQ > 0$). First of all transform variable Φ into new variable. So after this the new variable has been set the equation (38) will be modified as

$$i \frac{\partial}{\partial \tau} \varphi + P \frac{\partial^2}{\partial \xi^2} \varphi + Q e^{-2\Gamma\tau} \varphi |\varphi|^2 = 0. \quad (55)$$

we get following solution of dust-acoustic rogue waves of equation (38).

$$\Phi_1(\xi, \tau) = \sqrt{\frac{2|P|}{|Q|}} \left(\frac{4 + 16iP\zeta(\tau)\tau}{1 + 16(\eta(\tau)\tau)^2 + 4(\eta(\tau)\xi)^2} \right) \\ \times \exp \left[-i \frac{\Gamma\eta(\tau)\xi^2}{2P} \right] \sqrt{\eta(\tau)}. \quad (60)$$

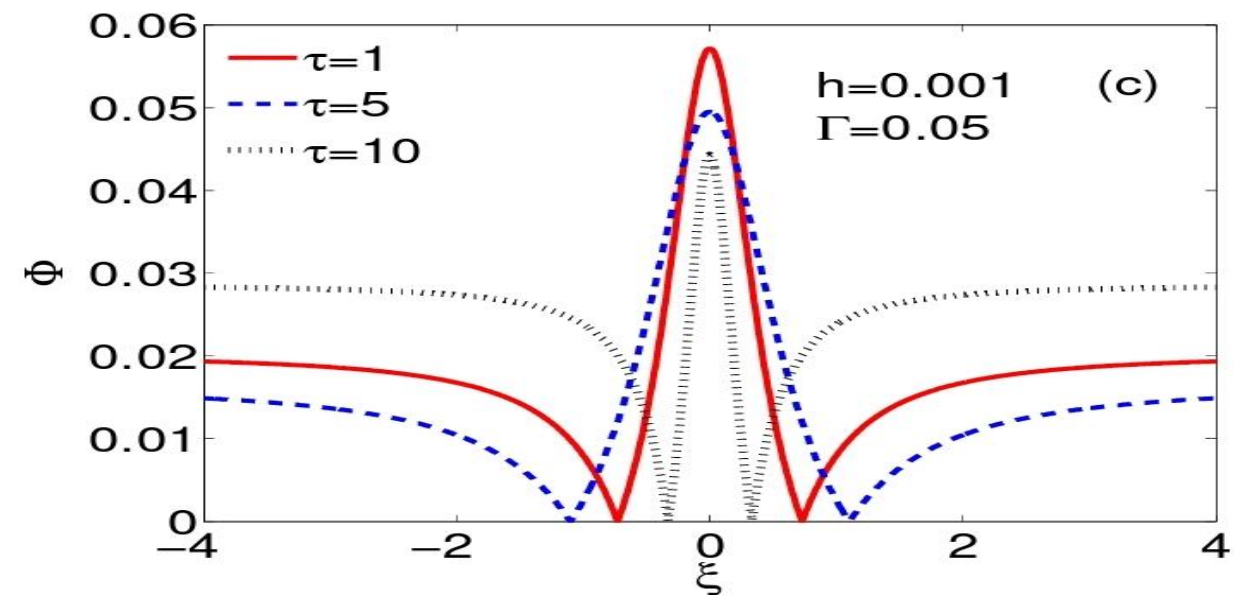
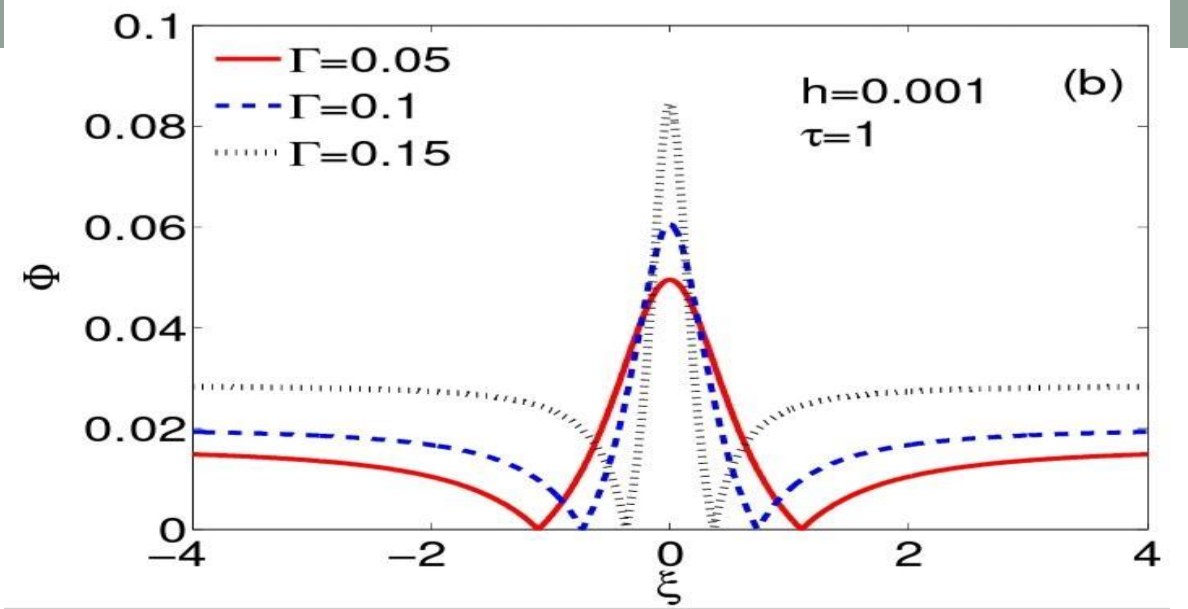
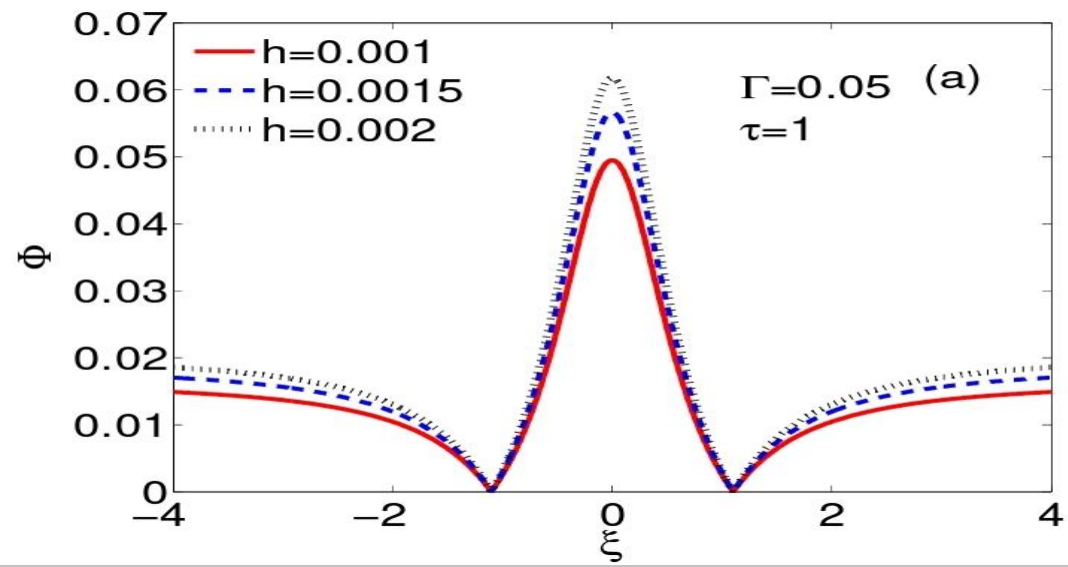


FIG. 7: Variation of dissipative dust-acoustic rogue waves solution of equation (60) at fixed value of wave vector $k = 2.5$ for different values of (a) Havnes function h , (b) collision parameter Γ and (c) time interval τ . Remaining plasma parameter are (a) $\Gamma = 0.05$ and $\tau = 1$, (b) $h = 0.001$ and $\tau = 1$ and (c) $h = 0.001$ and $\Gamma = 0.05$

Conclusion

The Dissipative nonlinear Schrodinger equation modified contribution of Havnes function h shows modulation instability. The instability region identified by $PQ > 0$ with contour plot of PQ on the (k,h) plane. Instability region begins at $k=2$ and get expanded with increasing dust concentration. Critical value K_{cr} for instability decreases exponentially with time interval and also decrease with increased dust concentration. The growth rate of the instability indicates a similar effects for both Havnes function (h) and time interval. The higher concentration of dust and the higher time interval effects decrease the growth rate.

The numerical solution of the dissipative NLS equation with condition $PQ > 0$ amplitude of solitons decreases with time interval. In the absence of dissipation width and amplitude of the solitons decreases and increases respectively with increasing h value. The bright and dark solitons width increases with the h effects. Both effects are behaving in a similar way. It is observed that the amplitude of the dissipative dust-acoustic rogue waves

References

1. F. F. Chen, “Introduction to Plasma Physics and Controlled Fusion”, New York, NY, USA: Plenum, 2nd ed, 1984.
2. M. Rosenberg, D. A. Mendis and V. W. Chow, “Weakly ionized cosmic gas: ionization and characterization”, *Astrophys. Space Sci.*, vol. 222, pp. 247–253, 1994.
3. Y. Nakamura, H. Bailung, and P. K. Shukla, “Observation of Ion-Acoustic Shocks in a Dusty Plasma”, *Phys. Rev. Lett.*, vol. 83, pp. 1602-1610, 1999.
4. F. Verheest, G. Manfred, A. Hellberg, and I. Kourakis, “Dust-ion-acoustic supersolitons in dusty plasmas with nonthermal electrons”, *Phys. Rev. E*, vol. 87, pp. 043107–043115, 2013.
5. V. Skarka, N. B. Aleksic, M. Derbazi, and V. I. Berezhiani, “Filamentation and coalescence of singular optical pulses in narrow-gap semiconductors and modeling of self-organization of vortex solitons using two-photon absorption”, *Phys. Rev. B*, vol. 81, pp. 035202–035211, 2010.

6. N. N. Rao, P. K. Shukla and M. Y. Yu, “Dust-acoustic waves in dusty plasmas”, *Planet. Space Sci.*, vol. 38, pp. 543–546, 1990.
7. A.. Barkan, N. D’Angelo and R. L. Merlino, “Laboratory experiments on ion cyclotron waves in a dusty plasma”, *Planet. Space Sci.*, vol. 43, pp. 905–908, 1995.
8. M. Irfan , S. Ali, A. Rahman, and A. M. Mirza, “Arbitrary amplitude oblique electrostatic solitary waves in a degenerate cold dusty magneto plasma”, *IEEE Trans. Plasma Sci.*, vol. 47, pp. 4151– 4158, 2019.
9. Y. N. Izvekova, Y. S. Reznichenko and S. I. Popel, “On the Possibility of Dust Acoustic Perturbation in Martian Ionosphere”, *Plasma Phys. Rep.*, vol. 46, pp. 1205–1209, 2020.
10. S.. K. Paul, N. A. Chowdhury, A. Mannan and A. A. Mamun, “Dust-acoustic rogue waves in non-thermal plasmas”, *Pramana – J. Phys.*, vol. 94, pp. 1935-1942, 2020.